JPET Fast Forward. Published on February 8, 2006 as DOI: 10.1124/jpet.105.095018
This article has not been copyedited and formatted. The final version may differ from this version.

DY-9760e is neuroprotective in rat microsphere embolism: Role of the cross-talk between calpain and caspase-3 through calpastatin.

Feng Han, Yasufumi Shirasaki, and Kohji Fukunaga

Department of Pharmacology, Graduate School of Pharmaceutical Sciences, Tohoku University, Sendai, Japan (F.H., K.F.); New Product Research Laboratories II, Daiichi Pharmaceutical Co., Ltd., Tokyo, Japan (Y.S.); and Tohoku University 21st Century COE Program “CRESCENDO” Sendai, Japan (F.H and K.F.)

a) Running title: Cross-talk between calpain and caspase-3 in ischemia

b) Correspondence should be addressed to Dr. Kohji Fukunaga, Department of Pharmacology, Graduate School of Pharmaceutical Sciences, Tohoku University, Aramaki-Aoba Aoba-ku, Sendai 980-8578, Japan; Tel.: 81-22 795-6836; fax: 81-22 795-6835
E-mail: **fukunaga@mail.pharm.tohoku.ac.jp**

c) 23 text pages, 0 tables, 8 figures, 38 references;
The number of words; Abstract, 176
Introduction, 517
Discussion, 1093

d) ABBREVIATIONS: DY-9760e, 3-[2-[4-(3-chloro-2-methylphenylmethyl)-1-piperazinyl]ethyl]-5,6-dimethoxy-1-(4-imidazolylmethyl)-1H-indazole dihydro-chloride 3.5 hydrate; CaM, calmodulin.

e) Neuropharmacology

JPET Fast Forward. Published on February 8, 2006 as DOI: 10.1124/jpet.105.095018
This article has not been copyedited and formatted. The final version may differ from this version.

ABSTRACT

Microsphere embolism (ME)-induced cerebral ischemia can elicit various pathological events leading to neuronal death. Western blotting and immunohistochemical studies revealed that expression of calpastatin, an endogenous calpain inhibitor, decreased following ME induction. Calpain activation following ME was apparently due in part to decrease in calpastatin in a late phase of neuronal injury. The time course of that decrease also paralleled caspase-3 activation. In vitro studies demonstrated that calpastatin was degraded by caspase-3 in a Ca^{2+}/calmodulin (CaM)-dependent manner. Since CaM binds directly to calpastatin, we asked whether a novel CaM antagonist, DY-9760e, inhibits caspase-3-induced calpastatin degradation during ME-induced neuronal damage. We also tested effect of DY-9760e on degradation of fodrin, a calpain substrate. Consistent with our hypothesis, DY-9760e (25mg/kg or 50mg/kg, i.p.) treatment inhibited degradation of calpastatin and fodrin in a dose-dependent manner. Since DY-9760e showed powerful neuroprotective activity with concomitant inhibition of calpastatin degradation, cross-talk between calpain and caspase-3 through calpastatin possibly accounts for ME-induced neuronal injury. Taken together, both inhibition of caspase-3-induced calpastatin degradation and calpain-induced fodrin breakdown by DY-9760e in part mediate its neuroprotective action.

JPET Fast Forward. Published on February 8, 2006 as DOI: 10.1124/jpet.105.095018
This article has not been copyedited and formatted. The final version may differ from this version.

Microspheres infused into the internal carotid artery induce small widespread embolisms, thereby leading to multiple infarct areas in the brain. The pathogenesis of microsphere embolism (ME)-induced brain damage resembles clinical features of human territorial stroke or brain vascular dementia (Demura et al, 1993). ME-induced ischemic injury includes many pathological events such as release of excitatory amino acids and deprivation of oxygen/glucose (Smith et al, 1990; Takeo et al, 1992). These events then trigger calcium influx into neurons, thereby leading to activation of Ca^{2+}-dependent signaling such as Ca^{2+}/CaM-dependent enzymes and Ca^{2+}-dependent proteases, calpains (Hayashi et al, 1998; Takagi et al, 2001). Brain ischemia/reperfusion injury is associated with calpain-induced proteolysis of the cytoskeleton including fodrin/spectrin (Fokuda et al, 1998; Sato et al, 1999; Yakota et al, 2003). We also documented nitric oxide production through activation of Ca^{2+}/CaM-dependent nitric oxide synthase (NOS) in ME-induced ischemia, thereby producing protein tyrosine nitration (Shirakura et al, 2005). The novel CaM inhibitor, DY-9760e, rescues neurons from ME-induced neuronal damage with concomitant inhibition of both NO production and protein tyrosine nitration (Hashiguchi et al, 2003). Interestingly, the neuroprotective effect of DY-9760e is also highly correlated with inhibition of calpain-induced breakdown of fodrin, a cytoskeletal and CaM-binding protein (Sato et al, 1999). Therefore, we hypothesize that inhibition of fodrin breakdown by calpain is partly involved in the neuroprotective action of DY-9760e.

In addition to calpain activation, caspase-3 plays pivotal roles in apoptotic cell death by inducing Bid and PARP activation (Affar et al, 2001;Degli Esposti et al, 2003). Inappropriate imbalances between calpain and calpastatin activation may play critical roles in the delayed neuronal death including apoptosis (Rami et al, 2003). Inhibition of nitric oxide production and fodrin breakdown by DY-9760e may suppress apoptotic signals such as caspase-3 activation through maintaining membrane integrity and suppressing mitochondrial damage. Indeed, cross-talk between calpain and caspase-3 has been documented in brain ischemia. For example, calpain-mediated N-terminal truncation of caspase-3 to a p30 polypeptide enhanced caspase-3 activation in one study (Blomgren, et al 2001) and inhibited its activation in another (McGinnis et al, 1999). Calpain-mediated N-terminal truncation of caspase-9 results in loss of ability to activate caspase-3 (Chua et al, 2000; Lankiewicz et al, 2000). Calpastatin, an endogenous

calpain inhibitor, is cleaved by caspase-3, thereby leading to loss of its inhibitory effect on calpain (Rami et al, 2003). Calpastatin also inhibits translocation of calpain to the plasma membrane, thereby inhibiting its proteolytic activity toward membranous cytoskeletal proteins such as fodrin (Melloni et al, 1996; Kosower et al, 2000). In addition, it is noteworthy that calpastatin is a CaM-binding protein, therefore it leads to the hypothesis that DY-9760e may be affects proteolysis of calpastatin in which mediated by caspase-3.

Little is known about cross-talk between calpain and caspase-3 in brain ischemia-induced neuronal death in vivo. Therefore, we asked whether cross-talk of calpain/caspase-3 participates in ME-induced neuronal damage through calpastatin. We also determined that DY-9760e has an inhibitory effect on calpastatin degradation during ischemia and show that inhibition of cross-talk between calpain and caspase-3 by DY-9760e likely underlies its neuroprotective action in brain ischemia. Therefore we propose a novel neuroprotective mechanism of DY-9760e.

JPET Fast Forward. Published on February 8, 2006 as DOI: 10.1124/jpet.105.095018
This article has not been copyedited and formatted. The final version may differ from this version.

Materials and Methods

A microsphere-induced permanent focal cerebral ischemic model

All experimental procedures using animals were approved by the Committee on Animal Experiments at Tohoku University. Male Wistar rats weighing 220-270g were subjected to general anesthesia induced by 4% halothane in oxygen, which was maintained by spontaneous breathing of 1.5% halothane in oxygen via a face mask. After placing animals in a supine position, a lateral longitudinal midline neck incision was performed to identify and dissect the left common carotid artery and separate the internal carotid artery from the external one at the bifurcation as the base point. Both external carotid and pterygopalatine arteries were temporarily occluded by aneurysm clips. One thousand non-radioactive microspheres (48.4 ± 0.7μm in diameter) suspended in a 20% dextran solution were injected with a 26 G needle into the left common carotid artery while visualizing flow into the internal carotid artery. The skin was closed and halothane anesthesia was terminated. Rectal temperature was monitored and maintained at 37 ± 0.5℃ with a heating blanket throughout the surgery. Sham-operated groups received the same treatment without microsphere injection. Behavioral changes such as lack of movement, truncal curvature and forced circling during locomotion following microsphere injection were observed as described (Miyake et al, 1993). Neurologic scores were determined 0.5, 24, 48 and 72 hours after microsphere injection. Scoring was as follows: grade 0, no deficit; grade 1, right side forelimb weakness and torso turning to the left side when held by tail; grade 2, circling to left side; grade 3, circling to left side and inability to bear weight on the right side; grade 4, no spontaneous locomotor activity. Rats with grade 0 and grade 4 were not used for subsequent experiments. Rats were decapitated at 2, 6, 12, 24, 48 and 72 hours after injection of microspheres and the striatum and cortical regions of the ipsilateral hemisphere were dissected for immunoblotting analyses.

Drug treatments

3-[2-[4-(3-chloro-2-methylphenylmethyl)-1-piperazinyl]ethyl]-5,6-dimethoxy-1-(4-imid azolylmethyl)-1H-indazole dihydro-chloride 3.5 hydrate (DY-9760e) was dissolved with

100 % DMSO and diluted in a 5 % glucose solution to a final concentration of 1 % DMSO. The microsphere-induced cerebral ischemic model was prepared as described above. After microsphere injection, rats were treated with DY-9760e at 12.5 mg/kg or 25 mg/kg intraperitoneally. In each case, DY-9760e was injected twice 30 minutes and 6 hours after microsphere injection. Vehicle-treated animals were administered the same volume of 1 % DMSO in 5 % glucose 30 minutes and 6 hours after microsphere injection, and sham groups received the same experimental procedures without microsphere injection. The dose of DY-9760e used did not affect the mean of arterial blood pressure monitored 30min after DY-9760e administration (data not shown).

Western blotting analysis

After decapitation, brains were removed and rinsed once with cold 0.32 M sucrose. Coronal sections of 2 mm were prepared by a hand brain slicer, and ipsilateral and contralateral hemispheres including cortex and striatum were dissected and stored at -80℃. Frozen brain tissues were homogenized in buffer containing 50 mM Tris-HCl (pH 7.4), 0.5% Triton X-100, 4 mM EGTA, 10 mM EDTA, 1 mM Na_3VO_4, 30 mM sodium pyrophosphate, 50 mM NaF, 100 nM calyculin A, 50 μg/ml leupeptin, 25 μg/ml pepstatin A, 50 μg/ml trypsin inhibitor and 1mM dithiothreitol (DTT). Insoluble material was removed by a 20-minutes centrifugation at 15,000g. After determining protein concentration in each fraction using Bradford's solution, samples containing equivalent amounts of protein were applied to 10%-15% acrylamide denaturing gel (SDS-PAGE) (Laemmli, 1970). Proteins were then transferred to an Immobilon PVDF transfer membrane for 2 hours at 70V. Membranes were blocked in 20 mM Tris-HCl (pH 7.4), 150 mM NaCl and 0.1% Tween 20 (TBS-T) containing 5% fat-free milk powder for 1 hour at room temperature and incubated with fodrin (rabbit polyclonal antibody; 1: 2000) (Sato et al, 1999), cleaved caspase-3 (rabbit polyclonal antibody; 1:1000, Cell Signaling Technology, Beverly, MA), calpastatin (goat polyclonal antibody; 1:500, Santa Cruz Biotechnology, Santa Cruz, CA), and β-tubulin (mouse monoclonal antibody; 1:10000, Sigma, St Louis, MO) antibodies overnight at 4℃. After washing, membranes were incubated 60 minutes at room temperature with the appropriate horseradish peroxidase (HRP)-conjugated secondary antibody diluted in TBS-T solution for 60 minutes at room temperature. Immunoreactive proteins were visualized with enhanced chemiluminescence detection system (Amersham Life Science,

Buckinghamshire, UK). Images were scanned and analyzed semiquantitatively using the Image Gauge Software (Fuji film, Tokyo, Japan).

Immunohistochemical studies

Rats were anesthetized and transcardially perfusion-fixed with 4 % paraformaldehyde in phosphate-buffered saline (PBS) as described (Kawano et al, 2002). Whole brains were immediately removed and post-fixed overnight at 4°C in the same fixative. Then, coronal brain sections at the coordinates of 1mm posterior to bregma (35-μm thick) were prepared using a vibratome. Sections were incubated at room temperature with 0.01% Triton-X100 in PBS for 30 minutes and for another hour in 3% bovine serum albumin (BSA) in PBS. For immunolabeling, slices were probed with anti-calpastatin (goat polyclonal antibody; 1:200; Santa Cruz Biotechnology), anti-cleaved caspase-3 (rabbit polyclonal antibody; 1:500; Cell Signaling Technology) and anti-NeuN (mouse monoclonal antibody; 1:500; Chemicon International, Temecula, CA) overnight at 4℃. After washing steps, sections were incubated with biotinylated anti-goat or rabbit IgG (1:5000) in TNB buffer for 1 hour, followed by both streptoavidin-HRP (1:5000) and Alexa 594 anti-mouse IgG (Molecular Probes, Eugene, OR, U.S.A.) in TNB buffer (1:400) and labeled for 2 hours. Sections were then stained with tetramethylrhodamine tyramide for 10 minutes using the TSA-Direct kit (NEN Life Science Products, Boston, MA). Immunofluorescent images were taken with a confocal laser scanning microscope (TCS SP, Leica Microsystems). To normalize immunoreactivity with anti-calpastatin antibody, we analyzed cortical slices without changing the confocal laser intensity and laser aperture. Furthermore, sections were double-stained with anti-NeuN antibody as a neuronal marker. We confirmed that the intensity of immunoreactivity with anti-NeuN antibody was the same between control and ischemic cortical slices. We further quantified the NeuN-positive neurons in six consecutive sections of the ipsilateral cortex under confocal laser microscope at 72h following ME to evaluate neuroprotective action of DY-9760e. The photographed regions are borders of the infarction, in which neither obvious morphological nor immunohistochemical changes with anti-NeuN antibody were observed in neurons as compared to sham-operated animals.

Capase-3 activity assay

Caspase-3 activity was measured by cleaving N-acetyl-Asp-Glu-Val-Asp-AMC

JPET Fast Forward. Published on February 8, 2006 as DOI: 10.1124/jpet.105.095018
This article has not been copyedited and formatted. The final version may differ from this version.

(7-amino-4-methylcoumarin) (BioMol, Plymonth Meeting, PA), a selective substrate for caspase-3. The ipsilateral hemisphere containing both striatum and cortex was obtained 24 hours after ischemia from both non-ischemic and ischemic groups. Tissues were homogenized in homogenizing buffer containing 15 mM Tris-HCl, pH 7.4, 320 mM sucrose, 1 mM EGTA, 2 mM EDTA, 50 mM NaF, 1 mM $MgCl_2$, 1 mM Na_3VO_4, and 30 mM sodium pyrophosphate plus protease inhibitors and centrifuged at 14,000 g for 60 minutes at 4℃. Protein concentration of supernatants was measured by Bradford's method, and equal amounts of proteins (100 μg) were incubated in a total volume of 400 μl comprised of 20 mM HEPES (pH 7.4), 10% glycerol, 2 mM DTT. The reaction was started by addition of caspase-3 fluorogenic substrate Ac-DEVD-AMC. After incubation for 60 minutes at 37℃, cleavage of the fluorogenic substrate was detected using a Perkin Elmer LS50B luminescence spectrometer with excitation and emission wavelengths of 380 and 460 nm, respectively. Activities of caspase-3 were expressed as changes in DEVDase activity.

Preparation of brain extracts and incubation with exogenous caspase-3 enzymes

Dissected brain tissue including cortex and striatum was homogenized in buffer containing 50 mM Tris-HCl, pH 7.4, 320 mM sucrose, 50μg/ml leupeptin, 25μg/ml pepstatin A, 50 μg/ml trypsin inhibitor, and 1mM DTT. After centrifugation at 15,000 g for 20 minutes, supernatants were incubated for 15 minutes in 60℃ to denature endogenous protease activities. Brain extracts (20μg protein) were incubated for 30 minutes with 0.2 μg purified caspase-3 at 30℃ in a 50μl-reaction medium containing 50 mM HEPES, 100 mM NaCl, 10 mM DTT, 1 mM EDTA and 10% glycerol. Under the same condition, heat-treated brain extracts were incubated with caspase-3 in the presence of 2.5, 5 or 20μM DY–9760e with or without Ca^{2+}/CaM. After incubation with purified caspase-3, brain extracts were subjected to SDS-PAGE, followed by immunoblotting with anti-calpastatin and anti-caspase-3 antibodies as described above.

Statistical analysis

Data were represented as means ± SD and obtained from at least four independent animals. Significance differences between treated and control animals at each time point were assessed by student's *t*–test. Multiple comparisons between experimental groups were performed by one-way analysis of variance (ANOVA), followed by Dunnett's test. $P < 0.05$ was considered significant.

Results

Proteolysis of fodrin and calpastatin following microsphere-induced cerebral ischemia

To verify temporal profile of calpain activation following ME, generation of a 150-kDa fodrin breakdown product (FBDP), which is specific breakdown product for calpain, was measured in rat brain following ME. A significant increase in FBDP was seen 2 hours after ME (Fig. 1A). Further significant increases in FBDP were also evident in 12-24 hours as compared with the amounts of FBDP at 6 hours. Immunoblotting analysis with β-tubulin showed an equal amount of loaded protein in each lane (Fig. 1A). To determine whether changes in expression of calpastatin, an endogenous calpain inhibitor, underlie further activation of calpain, calpastatin levels were assessed by immunoblotting using anti-calpastatin antibody. In sham-operated animals, a 110-kDa immunoreactive protein was detected by SDS-PAGE (Fig. 1B). Interestingly, levels of calpastatin were significantly reduced 6-24 hours after ME induction. Such decreased levels in calpastatin were correlated with further increases in FDBP generation seen after 12 hours, as shown in Fig. 1A.

Activation of caspase-3 accounts for calpastatin degradation

It is known that caspase-3 functions in the proteolysis of calpastatin. To confirm that reduced calpastatin levels after ME were due to activation of caspase-3, we assessed caspase-3 activity by immunoblotting analysis using antibody recognizing active 17 kDa caspase-3 or by measurement of caspase-3 activity. In brain extracts from the ipsilateral hemisphere containing the cortex and striatum, a significant increase in cleaved 17 kDa active caspase-3 protein was observed 6, 12 and 24 hours after ME induction (Fig.2A). Similarly, a persistent and significant increase in caspase-3 activity assessed by Ac-DEVD-AMC as substrate was observed 12–24 hours after ME induction (Fig.2B).

Effects of DY-9760e on the neurological deficits

Neurological sores were determined to verify the outcome of neurological functions at 0.5, 24, 48 and 72 hours after microsphere injection. There was no significant difference in scores between vehicle (2.90 ± 0.22) and DY-9760e-treated group (3.10 ± 0.42) at 0.5 hour after ME. However, the neurological scores in DY-9760e treated rats significantly improved at 24, 48 and 72 hours compared to vehicle-treated rats (Fig. 3).

JPET Fast Forward. Published on February 8, 2006 as DOI: 10.1124/jpet.105.095018
This article has not been copyedited and formatted. The final version may differ from this version.

Effects of DY-9760e on fodrin breakdown and calpastatin degradation following ME

Inhibition of fodrin breakdown by DY-9760e is due to inhibition of CaM binding to fodrin, which decreases its susceptibility to proteolysis by calpain. Therefore, we speculated that caspase-3-induced proteolysis of calpastatin possessing CaM-binding ability occurs in a Ca^{2+}/CaM-dependent manner and would be inhibited by DY-9760e. To confirm this possibility, rats were post-treated with DY-9760e and analyzed for effects on ME-induced calpastatin degradation as well as fodrin breakdown. Consistent with our hypothesis, proteolysis of calpastatin was significantly reduced by treatment with DY-9760e in a dose-dependent manner (Fig. 4A). Similarly, fodrin breakdown was inhibited by DY-9760e as reported in our previous study (Fig. 4B) (Sato et al, 1999).

DY-9760e treatment blocked activation of caspase-3 following ME

We next asked whether DY-9760e suppresses caspase-3 activation following ME. As shown in Fig. 5, the level of 17-kDa caspase-3 active fragment significantly increased 24 hours after ME, and post treatment with DY-9760e (25mg/kg and 50 mg/kg) inhibited increased active caspase-3 production in a dose-dependent manner (Fig. 5A). In accord with this, caspase-3 activity also increased at 24 hours after ME, as production of 17-kDa active fragment and increased activity was reduced by DY-9760e treatment (Fig. 5B).

Immunohistochemical calpastatin expression is reduced in neurons after ME-induced ischemia

To confirm that decreased calpastatin and caspase-3 activation occurs in neurons following ME, we performed immunohistochemical studies using anti-calpastatin and active caspase-3 antibodies. When cortical sections were double stained with anti-NeuN antibody, calpastatin immunoreactivity co-localized with NeuN immunoreactivity in both the cytosol and nucleus of cortical neurons (Fig. 6). Both immunoreactivities against calpastatin and NeuN markedly decreased 24 hours after ME in cortical neurons as compared to those seen in sham-operated animals. Immunoreactivity with calpastatin was markedly reduced even in surviving NeuN-positive neurons. Finally, treatment with DY-9760e partially restored immunostaining patterns against both calpastatin and NeuN. Like cortical neurons, decreased calpastatin immunoreactivity was also evident in striatal

JPET Fast Forward. Published on February 8, 2006 as DOI: 10.1124/jpet.105.095018
This article has not been copyedited and formatted. The final version may differ from this version.

neurons 24 hours after ME (data not shown). In contrast with decreased calpastatin immunoreactivity, dramatic increases in active caspase-3 immunoreactivity were observed in cortical neurons. The appearance of active caspase-3 in cortical neurons was largely abolished by treatment with DY-9760e, as expected. We further confirmed that DY-9760e treatment lead to a significantly increase in the number of survival neurons (825 ± 225 per mm^2; $P<0.05$) compared with vehicle group (542 ± 199 per mm^2) in the ipsilateral cortex 72 hours following ME.

Ca^{2+}/CaM-induced proteolysis of calpastatin by caspase-3 and its inhibition by DY-970e treatment

Finally, we confirmed that caspase-3 induced proteolysis of calpastatin in a Ca^{2+}/CaM dependent manner in vitro using purified caspase-3 and calpastatin in brain extracts. After inactivation of endogenous caspases and proteases by heating, brain extracts (20 μg) were incubated with or without purified caspase-3 in the presence or absence of Ca^{2+}/CaM and amounts of calpastatin were determined by immunoblotting. As shown in Fig. 7, addition of caspase-3 to the incubation medium resulted in proteolysis of 110-kDa calpastatin in a Ca^{2+}/CaM-dependent manner. Ca^{2+}/CaM-dependent proteolysis of calpastatin was inhibited by DY-9760e in a dose-dependent manner. To verify whether DY-9760e directly inhibits caspase-3 activity in vitro, we tested its effect on caspase-3 autolysis without substrate. The treatment with DY-9760e did not affect autolysis of caspase-3 up to 20 μM (data not shown).

Discussion

We recently introduced a novel neuroprotective drug, DY-9760e, ameliorating ischemia/reperfusion-induced neuronal damage (Sato et al., 1999; Hashiguchi et al., 2003). In the previous study, we defined two possible neuroprotective mechanisms of DY-9760e using brain ischemia/reperfusion models. DY-9760e is a potent CaM inhibitor that primary inhibits Ca^{2+}/CaM-depedent NOS (Hashiguchi et al., 2003) and fodrin breakdown (Sato et al., 1999) following ischemia/reperfusion in rat brain. Generation of NO following brain ischemia/reperfusion has detrimental effects on neurons by producing peroxynitrite (Hashiguchi et al., 2003). The fodrin breakdown likely mediates loss of membrane integrity, thereby leading to necrosis in neurons (Sato et al., 1999). Here, we found a novel mechanism of DY-9760e-induced neuroprotection, in which cross-talk between caspase-3 and calpain through calpastatin underlies its neuroprotective action. A key observation in the present study is that proteolysis of calpastatin by caspase-3 is dependent on Ca^{2+}/CaM in vivo. We also confirmed Ca^{2+}/CaM-dependent proteolysis of calpastatin in vitro by purified caspase-3 using brain extracts. We also found that DY-9760e, a novel neuroprotective agent, could rescue neurons in part by inhibiting cross-talk between caspase-3 and calpain following brain ischemia. Since cross-talk between caspase-3 and calpain plays crucial roles in apoptotic neuronal death following not only brain ischemia but also neurodegenerative disorders (Zhao et al, 2000; Blomgren et al, 2001; Pike et al, 2004), our results showing inhibition of this activity by a novel CaM antagonist is potentially important for development of novel neuroprotective drugs for these conditions.

Calpains are expressed as two isoforms (I or μ-calpain and II or m-calpain), which have different requirement for Ca^{2+} in the μM and mM ranges, respectively. μ-Calpain is known to function in both apoptotic and necrotic neuronal death following brain ischemia (Rami, 2000). In the case of apoptotic signaling, calpain-mediated cleavage of caspase-3, -7, -8, -9 and -12 is apparently involved in apoptotic signaling (Chua et al, 2000; Lankiewicz et al, 2000; Nakagawa et al, 2000; Blomgren et al, 2001). However, the functional relevance of cleavage of caspases by calpain is unclear. Calpain-mediated cleavage directly activated procaspase-7 and 12 (Ruiz-Vela et al, 1999; Nakagawa et al, 2000). In addition to the calpain-mediated caspases, caspase-mediated cleavage of calpastatin has been documented in cell culture models of apoptosis (Wang, et al, 1998; Porn-Ares et al, 1998; Kato et al, 2000; Neumar et al, 2003). Caspase-mediated

cleavage of calpastatin also results in activation of calpain. Therefore, the relevance of cross-talk between calpains and caspases should be tested in vivo ischemia models. We here show that caspase-mediated cleavage of calpastatin accounts for activation of calpain in an in vivo ischemia model. Furthermore, cleavage of calpastatin by caspase-3 occurred in a Ca^{2+}/CaM-dependent manner in the brain. Since calpastatin is ubiquitously expressed and is a potent inhibitor of μ- and m-calpain, the balance of calpain-calpastatin levels possibly controls pathological Ca^{2+}-induced events in mammalian tissues. Overexpression of calpastatin by gene transfer ameliorated contractile dysfunction in rat hearts subjected to ischemia/reperfusion (Maekawa et al., 2003). In rabbit hippocampus regions, μ-calpain is highly expressed in pyramidal neurons of both the CA1 and CA3 regions and studies of loss of calpastatin in CA1 pyramidal neurons suggest vulnerability of CA1 neurons to ischemic injury (Fukuda et al, 1990). A previous report also showed that calpastatin is proteolyzed by calpain in the rat hippocampus following ischemia/reperfusion (Saido et al, 1997). In the present study, both calpastatin and caspase-3 activation following ME was almost completely abolished by treatment with DY-9760e (50 mg/kg), whereas fodrin breakdown by calpain was partly inhibited DY-9760e treatment. Taken together, DY-9760e could preferentially inhibited Ca^{2+}/CaM-dependent calpastatin breakdown as compared to fodrin breakdown. Since the membrane-permeable calpain inhibitor MDL28,170 blocked brain injury in a rat model of focal stroke (Markraf et al, 1998), pathological activation of calpain likely leads to necrosis and apoptosis of neurons. On the other hand, physiological and transient activation of calpain in the limited compartment of the synapse is also essential for neuronal plasticity such as long-term potentiation (Jourdi et al, 2005). In our studies, caspase-3-mediated calpastatin degradation was closely associated with delayed increases in calpain activity, which were associated with irreversible neuronal death including apoptosis. Moreover, significant calpastatin degradation was observed 12 hours after ME induction. The delayed calpastatin degradation is particularly important concerning wide therapeutic time window for treatment of neuroprotective drugs.

Another interesting feature of the present study is finding that downstream targets of calpain and caspase-3, such as fodrin and calpastatin, respectively, are CaM binding proteins. Binding of Ca^{2+}/CaM to fodrin, which acts as a scaffold protein between ion channels and actin filaments promotes its degradation, thereby causing loss of membrane integrity and down-regulation of ion channel functions. The Ca^{2+}/CaM-mediated

susceptibility of fodrin to calpain is reduced by DY-9760e, which has potent neuroprotective action (Sato et al, 1999; Takagi et al, 2001; Hashiguchi et al, 2003). We believe that ME-induced ischemia causes early and mild activation of calpain by Ca^{2+} influx through glutamate receptors such as NMDA receptor (Fig. 8). The early calpain activation was evident 2 hours after ME induction, and likely leads to cleavage of caspase-3. Subsequently, Ca^{2+}/CaM accelerates calpastatin breakdown by the activated caspase-3. Thus, the inhibition of calpastatin proteolysis by DY-9760e treatment possibly accounts for suppression of further activation of calpain and caspase-3. Thus, we assumed that calpastatin is the key player in cross-talk between calpain and caspase-3, at least in rat ME-induced brain damage. In the rat transient forebrain ischemia model, calpain is predominantly activated 36-72 hours after ischemia without significant elevation of caspase-3 activity (Zhang et al, 2002). By contrast, we show here that ME-induced permanent ischemia causes marked increases in both calpain and caspase-3 activities 12 hours after ME induction. In particular, fodrin degradation by calpain was seen immediately after ME. Therefore, ME ischemic insults may induce aberrant and prolonged intracellular Ca^{2+} elevation as compared to transient forebrain ischemia, resulting in prolonged enhancement of the Ca^{2+}/CaM-dependent fodrin breakdown. In ischemic brain damage, caspase-3 is activated not only by calpain but also by activation of apoptotic signal through extracellular regulated signals such as Fas ligand and TNFα. Delayed calpain activation through caspase-3 mediated calpastatin degradation possibly turns on a switch leading to irreversible apoptotic or necrotic neuronal death.

In summary, our results provide evidence that caspase-3-mediated calpastatin proteolysis accounts for delayed and pronounced activation of calpain, thereby leading to irreversible neuronal death. Like transient forebrain ischemia, DY-9760e has a potent neuroprotective effect against ME-induced ischemic brain damage. In addition to inhibition of NOS activity by DY-9760e as described previously (Fukunaga et al, 2000; Hashiguchi et al, 2003), DY-9760e-mediated inhibition of fodrin and calpastatin degradation possibly contributes its neuroprotective action.

References

Affar EB, Germain M, Winstall E, Vodenicharov M, Shah RG, Salvesen GS, and Poirier GG (2001) Caspase-3-mediated processing of poly(ADP-ribose) glycohydrolase during apoptosis. *J Biol Chem* **276:**2935-2942.

Blomgren K, Zhu C, Wang X, Karlsson JO, Leverin AL, Bahr BA, Mallard C, and Hagberg H (2001) Synergistic activation of caspase-3 by m-calpain after neonatal hypoxia-ischemia: a mechanism of "pathological apoptosis"?. *J Biol Chem* **276:**10191-10198.

Chua BT, Guo K, and Li P (2000) Direct cleavage by the calcium-activated protease calpain can lead to inactivation of caspases. *J Biol Chem* **275:**5131-5135.

Degli Esposti M, Ferry G, Masdehors P, Boutin JA, Hickman JA, and Dive C (2003) Post-translational modification of Bid has differential effects on its susceptibility to cleavage by caspase 8 or caspase 3. *J Biol Chem* **278:**15749-15757.

Demura N, Mizukawa K, Ogawa N, Yamashita K, and Kanazawa I (1993) A cerebral ischemia model produced by injection of microspheres via the external carotid artery in freely moving rats. *Neurosci Res* **17:**23-30.

Fukuda S, Harada K, Kunimatsu M, Sakabe T, and Yoshida K (1998) Postischemic reperfusion induces alpha-fodrin proteolysis by m-calpain in the synaptosome and nucleus in rat brain. *J Neurochem* **70:**2526-2532.

Fukuda T, Adachi E, Kawashima S, Yoshiya I, and Hashimoto PH (1990) Immunohistochemical distribution of calcium-activated neutral proteases ans endogenous CANP inhibitor in the rabbit hippocampus. *J Comp Neurol* **302:** 100-109.

Fukunaga K, Ohmitsu M, Miyamoto E, Sato T, Sugimura M, Uchida T, and Shirasaki Y (2000) Inhibition of neuronal nitric oxide synthase activity by 3-[2-[4-(3-chloro-2-methylphenyl)- 1-piperazinyl]ethyl]-5, 6-dimethoxy-1-(4-imidazolylmethyl)-1H-indazole dihydrochloride 3.5 hydrate (DY-9760e), a novel neuroprotective agent, in vitro and in cultured neuroblastoma cells in situ. *Biochem Pharmacol* **60:**693-699.

Hashiguchi A, kawano T, Yano S, Morioka M, Hamada J, Sato T, Shirasaki Y, Ushio Y, and Fukunaga K (2003) The neuroprotective effect of a novel calmodulin antagonist, 3-[2-[4-(3-chloro-2-methylphenyl)-1-piperazinyl]ethyl]-5,

6-dimethoxy-1-(4-imidazolylmethyl)-1H-indazole dihydrochloride 3.5 hydrate, in transient forebrain ischemia. *Neuroscience* **121:** 379-386.

Hayashi H, Sato K, Kuruhara Y, and Takeo S (1998) Microsphere embolism-induced changes in noradrenaline release in the cerebral cortex in rats. *Brain Res* **783:**241-248.

Jourdi H, Yanagihara T, Martinez U, Bi X, Lynch G, and Braudry M (2005) Effects of positive AMPA receptor modulators on calpain-mediated spectrin degradation in cultured hippocampal slices. *Neurochem Int* **46:**31-40.

Kato M, Nonaka T, Maki M, Kikuchi H, and Imajoh-Ohmi S (2000) Caspases cleave the amino-terminal calpain inhibitory unit of calpastatin during apoptosis in human Jurkat T cells. *J Biol Chem* **127:**297-305.

Kawano T, Morioka M, Yano S, Hamada J, Ushio Y, Miyamoto E, and Fukunaga K (2002) Decreased Akt activity is associated with activation of forkhead transcription factor after transient forebrain ischemia in gerbil hippocampus. *J Cereb Blood Flow Metab* **22:**926-934.

Kosower NS and Barnoy S (2000) Calpastatin (the endogenous calpain inhibitor) and membrane protein degradation in cell fusion. *Methods Mol Biol* **144:**181-194

Laemmli UK (1970) Cleavage of structure proteins during the assembly of the head of bacteriophage T4. *Nature* **227:**680-685.

Lankiewicz S, Marc Luetjens C, Truc Bui N, Krohn AJ, Poppe M, Cole GM, Saido TC, and Prehn JH (2000) Activation of calpain I converts excitotoxic neuron death into a caspase-independent cell death. *J Biol Chem* **275:**17064-17071.

Maekawa A, Lee J K, Nagaya T, Kamiya K, Yasui K, Horiba M, Miwa K, Uzzaman M, Maki M, Ueda Y, and Kodama I (2003) Overexpression of calpastatin by gene transfer prevents troponin I degradation and ameliorates contractile dysfunction in rat hearts subjected to ischemia/reperfusion. *J Mol Cell Cardiol* **35:**1277-1284.

Markgraf CG, Velayo NL, Johnson MP, McCarty DR, Medhi S, Koehl JR, Chmielewski PA, and Linnik MD (1998) Six-hour window of opportunity for calpain inhibition in focal cerebral ischemia in rats, *Stroke* **29,** 152-153.

McGinnis KM, Gnegy ME, Park YH, Mukerjee N, and Wang KK (1999) Procaspase-3 and poly(ADP)ribose polymerase (PARP) are calpain substrates. *Biochem Biophys Res Commun* **263:**94-99.

Melloni E, Michetti M, Salamino F, Minafra R, and Pontremoli S (1996) Modulation of

the calpain autoproteolysis by calpastatin and phospholipids. *Biochem Biophys Res Commun* **229:**193-197.

Miyake K, Takeo S, and Kajihara H (1993) Sustained decrease in brain regional blood flow after microsphere embolism in rats. *Stroke* **24,** 415-420.

Nakagawa T and Yuan J (2000) Cross-talk between two cysteine protease families. Activation of caspase-12 by calpain in apoptosis. *J Cell Biol* **150:**887-894.

Neumar RW, Xu YA, Gada H, Guttmann RP, and Siman R (2003) Cross-talk between calpain and caspase proteolytic systems during neuronal apoptosis. *J Biol Chem* **278:**14162-14167.

Pike BR, Flint J, Dave JR, Lu XC, Wang KK, Tortella FC, and Hayes RL (2004) Accumulation of calpain and caspase-3 proteolytic fragments of brain-derived alphaII-spectrin in cerebral spinal fluid after middle cerebral artery occlusion in rats. *J Cereb Blood Flow Metab* **24:**98-106.

Porn-Ares MI, Samali A, and Orrenius S (1998) Cleavage of the calpain inhibitor, calpastatin, during apoptosis. *Cell Death Differ* **5:**1028-1033.

Rami A, Agarwal R, Botez G, and Winckler J (2000) mu-Calpain activation, DNA fragmentation, and synergistic effects of caspase and calpain inhibitors in protecting hippocampal neurons from ischemic damage. *Brain Res* **866:**299-312.

Rami A, Volkmann T, Agarwal R, Schoninger S, Nurnberger F, Saido TC, and Winckler J (2003) beta2-Adrenergic receptor responsiveness of the calpain-calpastatin system and attenuation of neuronal death in rat hippocampus after transient global ischemia. *Neurosci Res* **47:**373-382.

Ruiz-Vela A, Gonzalez de Buitrago G, and Martinez-AC (1999) Implication of calpain in caspase activation during B cell clonal deletion. *EMBO J* **18:**4988-4998.

Sato T, Morishima Y, Sugimura M, Uchida T, and Shirasaki Y (1999) DY-9760e, a novel calmodulin antagonist, reduces brain damage induced by transient focal cerebral ischemia. *Eur J Pharmacol* **370:**117-123.

Saido TC, Kawashima S, Tani E, and Yokota M (1997) Up- and down-regulation of calpain inhibitor polypeptide, calpastatin, in postischemic hippocampus. *Neurosci Lett* **227:** 75-78.

Shirakura T, Han F, Shiota N, Moriguchi S, Kasahara J, Sato T, Shirasaki Y and Fukunaga K (2005) Inhibition of Nitric Oxide Production and Protein Tyrosine Nitration Contribute to Neuroprotection by a Novel Calmodulin Antagonist, DY-9760e, in

the Rat Microsphere Embolism. *Biol Pharm Bull* **28:**1658-1661.

Smith CD, Thomas GS, Kryscio RJ, and Markesbery WR (1990) ^{31}P spectroscopy in experimental embolic stroke: correlation with infarct size. *NMR Biomed* **3:**259-264.

Takagi K, Sato T, Shirasaki Y, Narita K, Tamura A, and Sano K (2001) Post-ischemic administration of DY-9760e, a novel calmodulin antagonist, reduced infarct volume in the permanent focal ischemia model of spontaneously hypertensive rat. *Neurol Res* **23:**662-668.

Takeo S, Taguchi T, Tanonaka K, Miyake K, Horiguchi T, Takagi N, and Fujimori K (1992) Sustained damage to energy metabolism of brain regions after microsphere embolism in rats. *Stroke* **23:**62-68.

Wang KK, Posmantur R, Nadimpalli R, Nath R, Mohan P, Nixon RA, Talanian RV, Keegan M, Herzog L, and Allen H (1998) Caspase-mediated fragmentation of calpain inhibitor protein calpastatin during apoptosis. *Arch Biochem Biophys* **356:**187-196.

Yokota M, Saido TC, Kamitani H, Tabuchi S, Satokata I, and Watanabe T (2003) Calpain induces proteolysis of neuronal cytoskeleton in ischemic gerbil forebrain. *Brain Res* **984:**122-132.

Zhang C, Siman R, Xu YA, Mills AM, Frederick JR, and Neumar RW (2002) Comparison of calpain and caspase activities in the adult rat brain after transient forebrain ischemia. *Neurobiol Dis* **10:**289-305.

Zhao X, Newcomb JK, Pike BR, Wang KK, d'Avella D, and Hayes RL (2000) Novel characteristics of glutamate-induced cell death in primary septohippocampal cultures: relationship to calpain and caspase-3 protease activation. *J Cereb Blood Flow Metab* **20:**550-562.

JPET Fast Forward. Published on February 8, 2006 as DOI: 10.1124/jpet.105.095018
This article has not been copyedited and formatted. The final version may differ from this version.

Figure Legends

Fig. 1. Changes in expression of fodrin and calpastatin following ME induction in rat brain. (A) Calpain-mediated degradation of fodrin was determined by quantifying the 150-kDa fodrin breakdown product (FBDP) after ME induction. The striatum and cortical regions of the ipsilateral hemisphere were dissected for immunoblotting analysis at the indicated times. Immunoblots with anti-β-tubulin antibody showed equal protein loading. Quantitative analysis of the 150-kDa FBDP levels was performed by densitometric analysis of immunoblots. Data are expressed as percentage of values of sham-operated animals (mean ± SD, n=4). $^{*}P<0.05$ $^{**}P<0.01$ versus sham-operated group. $^{\#}P<0.05$ versus the 6-hours group. **(B)** Representative image of immunoblot using anti-calpastatin antibody and the same samples described above. Quantitative analysis of the 110-kDa calpastatin levels was performed by densitometric analysis of immunoblots. Data are expressed as percentage of values of sham-operated animals (mean ± SD, n=4). $^{*}P<0.05$, $^{**}P<0.01$ versus sham-operated animals. $^{\#}P<0.05$ versus the 6-hours group.

Fig. 2. Changes in levels of 17-kDa active caspase-3 following ME induction. (A) Representative immunoblots showing temporal changes in the 17-kDa active caspase-3 fragment following ME. Quantitative analysis of the 17-kDa active caspase-3 levels was performed by densitometric analysis of immunoblots. Data are expressed as percentage of values of sham-operated animals (mean ± SD, n=4). $^{*}P<0.05$, $^{**}P<0.01$ versus sham-operated animals. **(B)** Caspase-3 activity in brain extracts was assessed using N-acetyl-Asp-Glu-Val-Asp-AMC (7-amino-4-methylcoumarin) as a substrate. Caspase-3 activities were represented as percentage of values of sham-operated animals. Data are presented as mean ± SD (n=4), $^{*}P<0.05$ versus sham-operated group.

Fig. 3. Effects of DY-9760e on the neurological deficits. DY-9760e (12.5 mg/kg) was administered intraperitoneally twice 30 minutes and 6 hours after ME induction. Neurological score was determined 0.5, 24, 48 and 72 hours after ME with or without DY-9760e post-treatment. Data presented as mean ± SD (n=6), $^{\#}P<0.05$, $^{\#\#}P<0.01$ versus vehicle-treated rats.

Fig. 4. Effects of post-ischemic treatment with DY-9760e on calpastatin degradation and fodrin breakdown. DY-9760e (12.5 or 25 mg/kg) was administered

JPET Fast Forward. Published on February 8, 2006 as DOI: 10.1124/jpet.105.095018
This article has not been copyedited and formatted. The final version may differ from this version.

intraperitoneally twice 30 minutes and 6 hours after ME induction. **(A)** Representative image of immunoblot using an anti-calpastatin antibody. Quantitative analysis of levels of 110-kDa calpastatin protein was performed by densitometric analysis of immunoblots. Data are expressed as percentage of values of sham-operated animals (mean ± SD, n=5). $^{**}P<0.01$ versus sham-operated animals; $^{\#}P<0.05$, $^{\#\#}P<0.01$ versus vehicle-treated rats. **(B)** Representative image of immunoblot using the anti-150-kDa FBDP antibody. Quantitative analysis of 150-kDa FBDP levels was performed by densitometric analysis of immunoblots. Data are expressed as percentage of values of sham-operated animals (mean ± SD, n=4). $^{**}P<0.01$ versus sham-operated rats. $^{\#}P<0.05$, $^{\#\#}P<0.01$ versus vehicle-treated rats.

Fig. 5. Inhibitory effects of DY-9760e on ME-induced caspase-3 activation. (A) Cleaved active caspase-3 was measured 24 hours after ME by immunoblotting with or without post-treatment with DY-9760e. Quantitative analysis of 17-kDa cleaved caspase-3 levels was performed by densitometric analysis of immunoblots. Data are expressed as percentage of values of sham-operated animals (mean ± SD, n=5). $^{**}P<0.01$ versus sham-operated rats. $^{\#}P<0.05$, $^{\#\#}P<0.01$ versus vehicle-treated rats. **(B)** Activity of caspase-3 assessed by N-acetyl-Asp-Glu-Val-Asp-AMC cleavage. DY-9760e significantly suppressed elevated caspase-3 activity 24 hours after ME. Data presented as mean ± SD (n=4), $^{*}P<0.05$ versus sham-operated rats. $^{\#}P<0.05$ versus vehicle-treated rats.

Fig. 6. Immunohistochemical localization of calpastatin and active caspase-3 in the cortex. (A) Confocal microscopic images of double staining with anti-calpastatin (green fluorescence) and anti-NeuN (red fluorescence) antibodies, indicating predominant expression of calpastatin in neurons stained with anti-NeuN antibody. Markedly decreased calpastatin immunoreactivity was observed in cortex 24 hours after ME. Calpastatin degradation in neurons was blocked by DY-9760e treatment. **(B)** Double staining with anti-active caspase-3 (green fluorescence) and anti-NeuN (red fluorescence) antibodies in the cortex showed that activation of caspase-3 occurred primarily in neurons of ME rats. The number of cells showing increases in active caspase-3 was significantly reduced by DY-9760e treatment. Scale bar = 30 μm.

Fig. 7. Inhibition of caspase-3 mediated calpastatin degradation by DY-9760e in rat brain extracts. Brain extracts containing endogenous calpastatin were incubated with recombinant caspase-3 in the presence or absence of Ca^{2+}/CaM. The incubation was also performed in the presence or absence of DY-9760e. Calpastatin protein levels were measured by immunoblotting. Representative image of immunoblot using anti-110-kDa calpastatin antibody. Quantitative analysis of the 110-kDa calpastatin levels was performed by densitometric analysis of immunoblots. Data are expressed as percentage of values of EGTA (mean ± SD, n=4). $^{*}P<0.05$ versus EGTA treatment. $^{\#}P<0.05$ versus Ca^{2+}/CaM plus caspase-3 treatment.

Fig. 8. Schematic model of Ca^{2+} signaling underlying neuronal death and possible site of action of DY-9760e. We have shown that Ca^{2+} elevation by NMDA activation promotes calpain activation (1). The earlier activation of calpain results in cleavage of caspase-3, leading to its activation (2). Cleaved caspase-3 mediates degradation of calpastatin in the presence of Ca^{2+}/CaM (3). The calpastatin degeneration further promotes calpain activation (4) and accelerates caspase–3 cleavage (5) during ME ischemia. In addition to inhibiting fodrin breakdown, DY-9760e inhibits Ca^{2+}/CaM-dependent calpastatin degradation, thereby eliminating delayed and marked activation of calpain, which is critical for activating apoptosis signals.

JPET Fast Forward. Published on February 8, 2006 as DOI: 10.1124/jpet.105.095018
This article has not been copyedited and formatted. The final version may differ from this version.

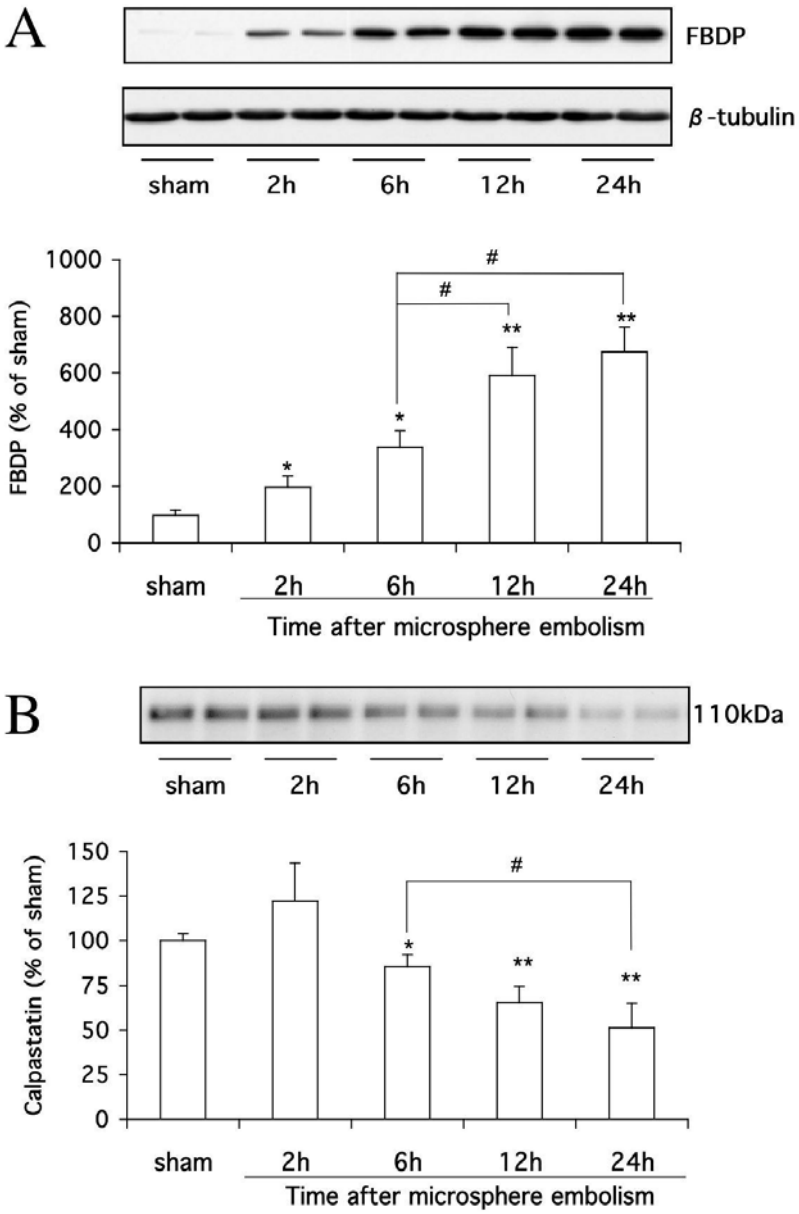

Fig.1.

JPET Fast Forward. Published on February 8, 2006 as DOI: 10.1124/jpet.105.095018
This article has not been copyedited and formatted. The final version may differ from this version.

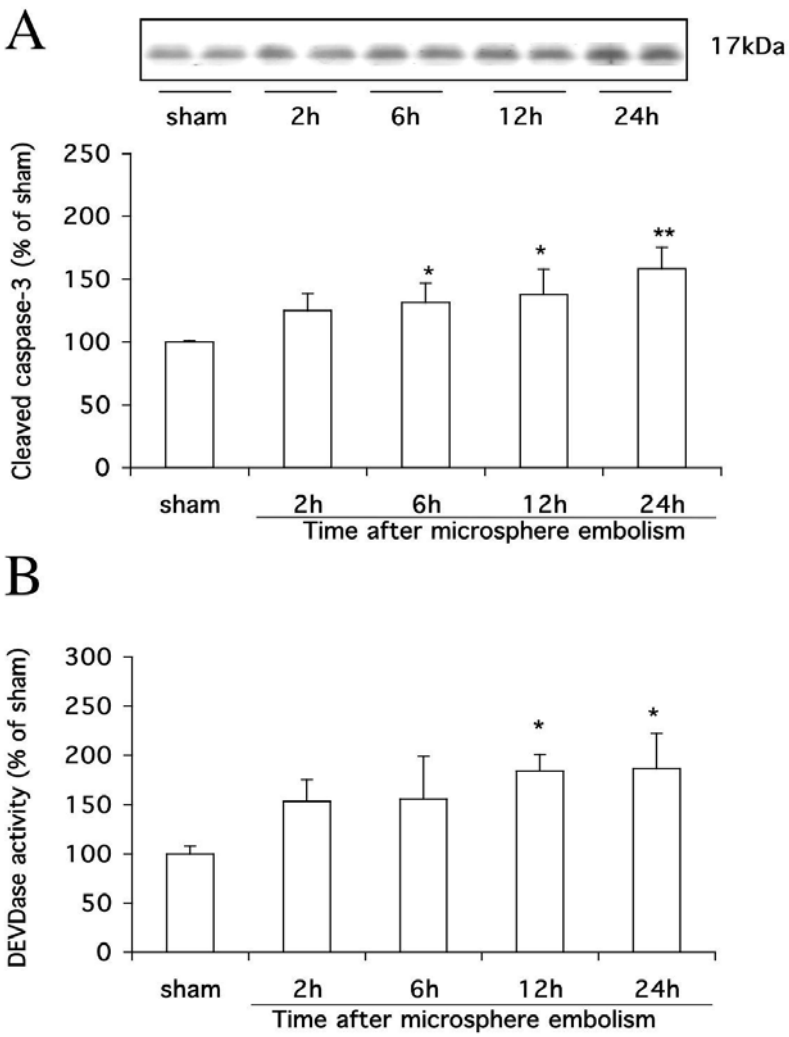

Fig.2.

JPET Fast Forward. Published on February 8, 2006 as DOI: 10.1124/jpet.105.095018
This article has not been copyedited and formatted. The final version may differ from this version.

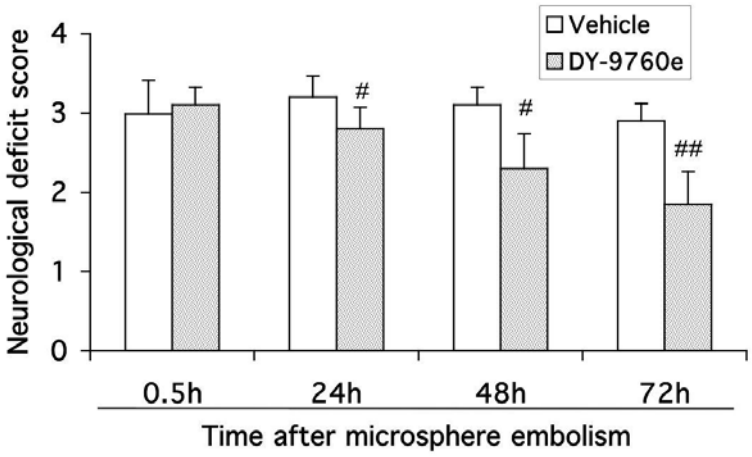

Fig.3.

JPET Fast Forward. Published on February 8, 2006 as DOI: 10.1124/jpet.105.095018
This article has not been copyedited and formatted. The final version may differ from this version.

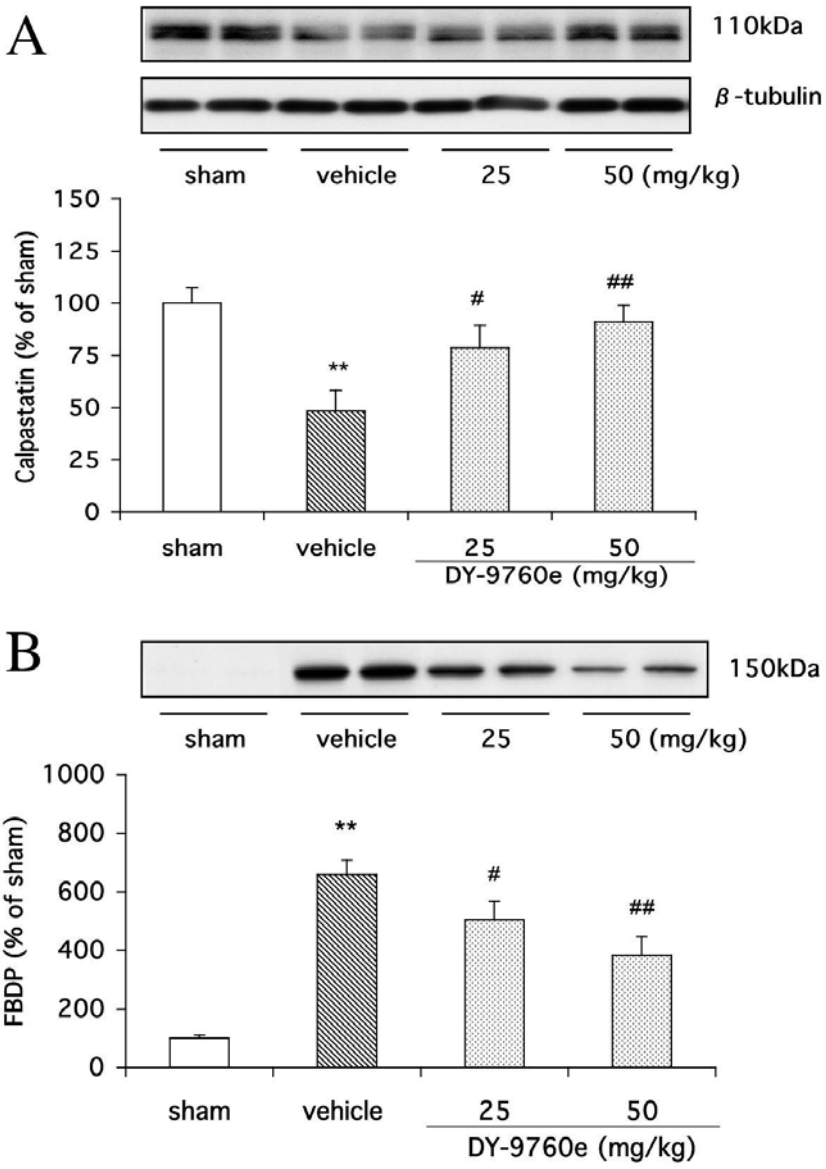

Fig.4.

JPET Fast Forward. Published on February 8, 2006 as DOI: 10.1124/jpet.105.095018
This article has not been copyedited and formatted. The final version may differ from this version.

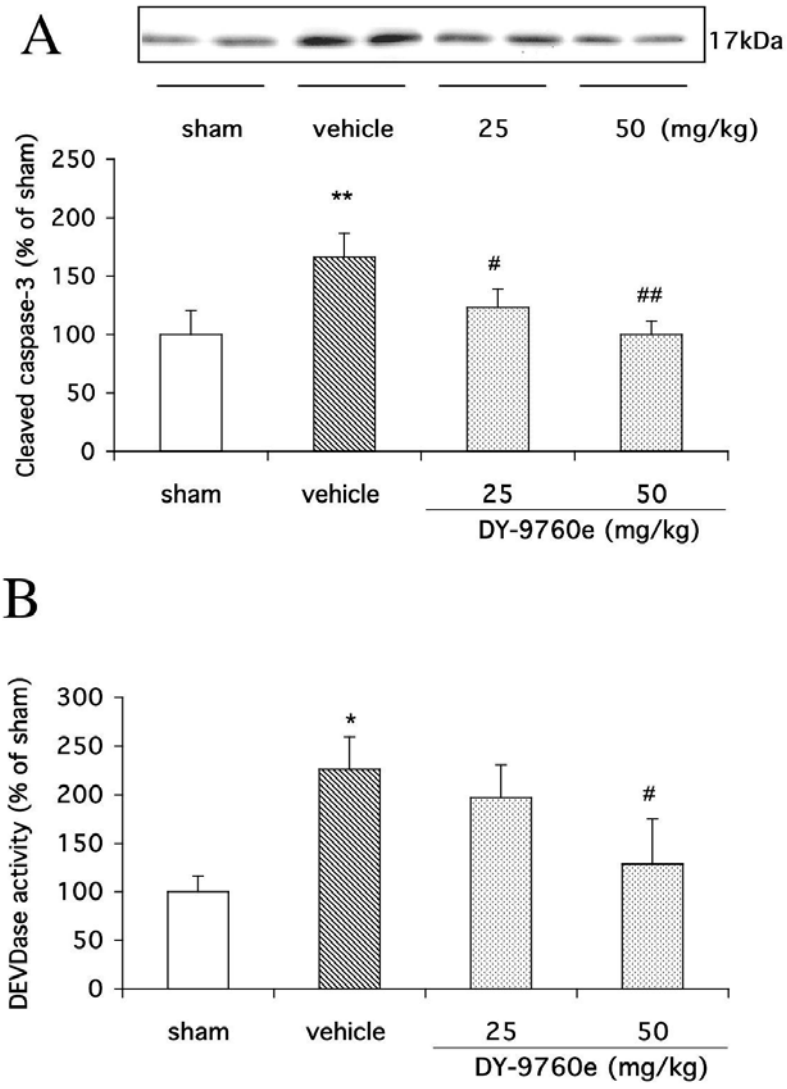

Fig.5.

JPET Fast Forward. Published on February 8, 2006 as DOI: 10.1124/jpet.105.095018
This article has not been copyedited and formatted. The final version may differ from this version.

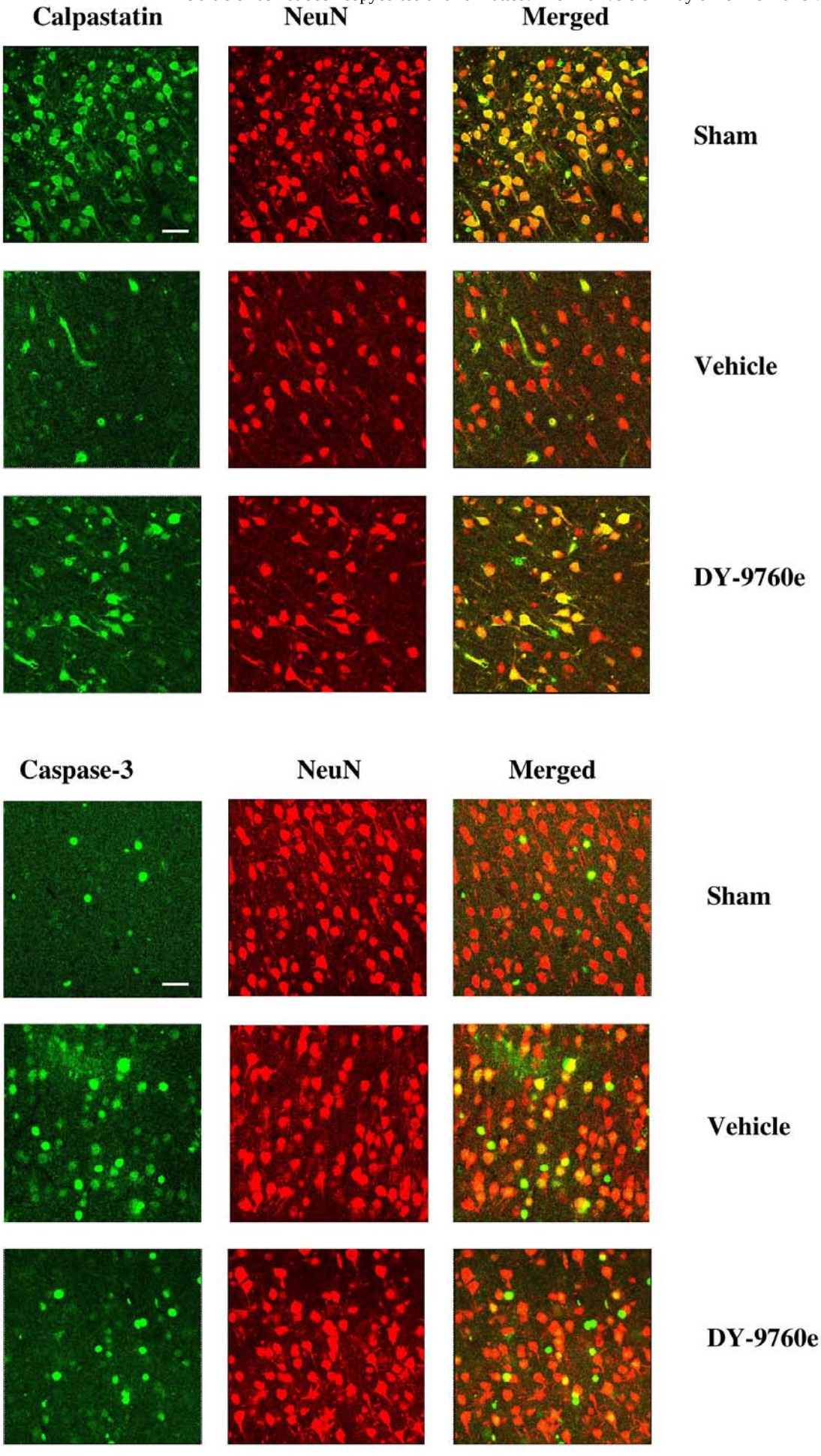

Fig.6.

JPET Fast Forward. Published on February 8, 2006 as DOI: 10.1124/jpet.105.095018
This article has not been copyedited and formatted. The final version may differ from this version.

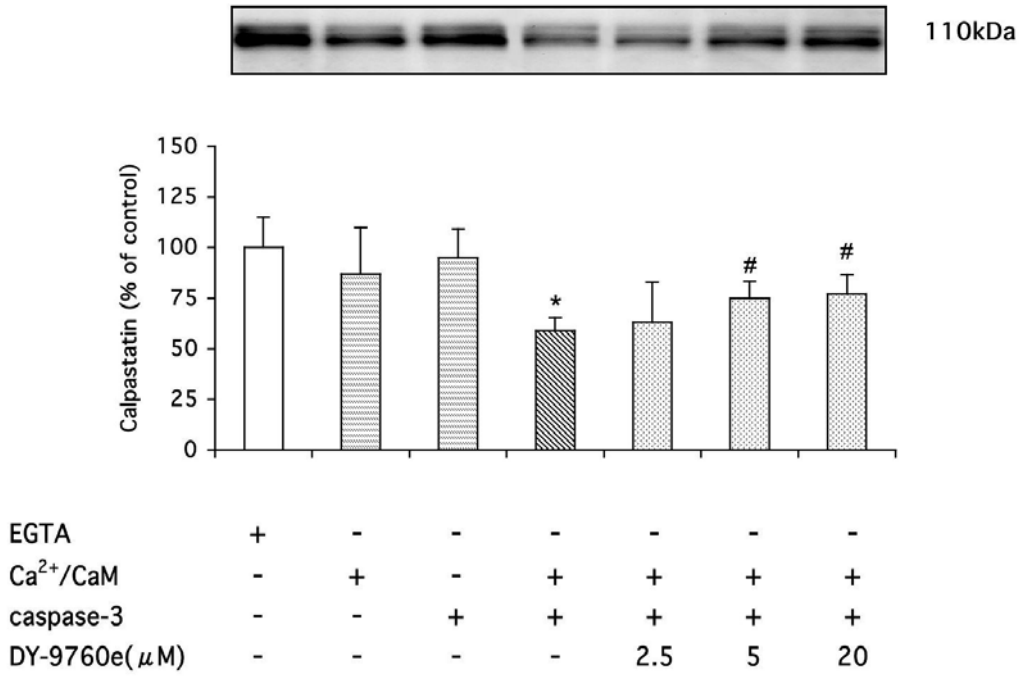

Fig.7.

JPET Fast Forward. Published on February 8, 2006 as DOI: 10.1124/jpet.105.095018
This article has not been copyedited and formatted. The final version may differ from this version.

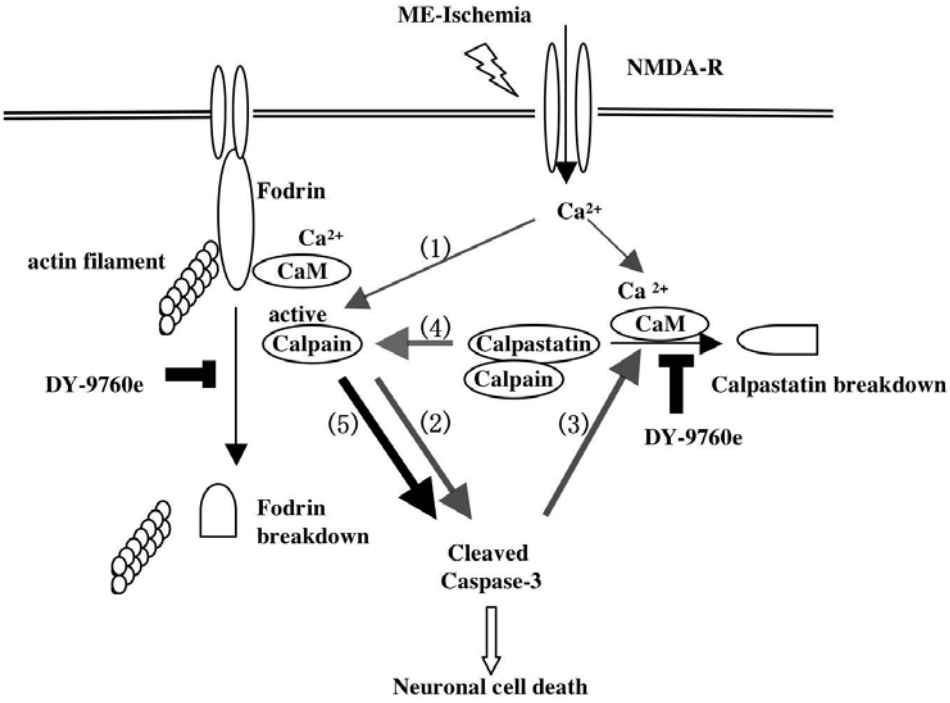

Fig.8.